AIAA 80-1671R

Orbit Selection for the Stanford Relativity Gyroscope Experiment

R. Vassar,* J.V. Breakwell,† C.W.F. Everitt,‡ and R.A. VanPatten§
Stanford University, Stanford, Calif.

This paper discusses an error analysis for the Stanford Relativity Gyroscope experiment, designed to measure the precession of a gyroscope's spin axis predicted by General Relativity. Measurements will be made of the spin-axis orientations of four superconducting spherical gyroscopes carried by an Earth satellite. Two relativistic precessions are predicted: a "geodetic" precession associated with the satellite's orbital motion and a "motional" precession due to the Earth's rotation. The error in determining the relativistic precession rates was computed using a Kalman filter covariance analysis with a realistic error model. Studies show that a slightly off-polar orbit is better than a polar orbit for determining the "motional" drift.

Introduction

IN 1960, Schiff[1,2] predicted using Einstein's General Theory of Relativity that a gyroscope in orbit about the Earth would experience a precession of its spin axis relative to the "fixed stars." Two relativistic precessions are predicted: a "geodetic" precession associated with the orbital motion of the gyro about the Earth and a "motional" precession due to the Earth's rotation. Figure 1 shows the two effects for a gyro in a 520-km altitude polar orbit with its spin axis in the equatorial and orbital planes. The geodetic precession is north approximately 6.9 arcsecond/year and the motional precession is east approximately 0.044 arcsecond/year. For a gyro in a nonpolar-inclined orbit these precessions include terms which vary sinusoidally with the longitude of the orbit's ascending node relative to the gyro spin axis.

The Standford Relativity Gyroscope experiment as presently envisioned will have four superconducting electrostatically suspended spherical gyros carried by a drag-free Earth satellite. A drag-free statellite uses thrusters to continually counteract the effects of air drag and solar radiation pressure and thus the satellite follows a true gravitational trajectory. The drag-free orbital environment was chosen to reduce suspension forces which result in torques, down to a level where the relativistic precessions can be measured. Four gyros will be carried to provide redundancy and to allow the gyros to be oriented in pairs with their spin axes antiparallel. The gyros are electrostatically suspended since the desired drift performance (<1 milliarcsecond/year) is not obtainable with a gimballed suspension system. The experiment will be cryogenic to take advantage of the stability of materials at a few degrees kelvin and also so a property of a spinning superconductor can be used to measure the spin-axis orientation relative to the satellite. By this property a spinning superconductor will generate a small magnetic field, called the London moment, aligned with its instantaneous spin axis.

The plan is to use Rigel, which is 8 deg south of the celestial equator, as an "inertial" reference with respect to which to measure the precession of the gyro. The gyros will be spun up with their spin axes initially approximately parallel or antiparallel to the line of sight to Rigel. A telescope will be used to point the spacecraft at Rigel. Each spin-axis orientation with respect to the spacecraft is measured by using a SQUID magnetometer to read out the direction of the London moment. The magnetometer is shielded from the Earth's magnetic field by a large superconducting lead bag around the entire experiment package. The orientation with respect to the satellite is compared with the telescope indication of the direction of Rigel to get the inertial orientation. For more information on the experiment see Refs. 3-8.

To measure the small relativistic precessions to a high accuracy (e.g., ±1 milliarcsecond/year) all extraneous error sources must be corrected for or else reduced to an acceptable level. Some error torques are effectively averaged to an acceptable level by rolling the satellite about the line of sight to Rigel with a period of 10 to 15 min.

Relativistic Precessions

Table 1 gives the relativistic precessions predicted by general relativity. δ is the declination of the star and i is the inclination of the orbit plane, Ω is the longitude of the ascending node relative to the guide star, $\Omega_0 = \Omega(t=0)$, $\omega_n = -\dot{\Omega} = (3/2)J_2(R_\oplus/a)^2 n \cos i$, where J_2 is the Earth's oblateness coefficient, A_G is the geodetic coefficent, and A_M is the motional coefficient. A_G is predicted to be about 6.9 arcsecond/year and A_M is predicted to be about 44 milliarcsecond/year in a 520-km altitude orbit.

Table 2 shows the simplification that results in a polar orbit (i.e., $i=90°$, $\Omega=\Omega_0$).

Errors in the Experiment

There are three major error sources in the experiment. They are as follows:

1) precessions due to nonrelativistic torques (i.e., torques due to the electrostatic suspension system acting on a rotor which is not perfectly spherical or torques due to the center of mass being offset from the center of support);

2) measurement errors (i.e., noise and scale factor error associated with the SQUID magnetometer measurement of the gyro spin-axis orientation; noise in the star blipper measurement of roll angle); and

3) uncertainty in the "inertial" reference (i.e., unknown proper motion of the guide star, Rigel).

A Kalman filter covariance analysis was performed to analyze the effect of these errors on our determination from a single gyro of A_G and A_M at the end of a 1-yr mission. In order to perform the covariance analysis, realistic measurement models had to be developed.

Presented as Paper 80-1671 at the AIAA/AAS Astrodynamics Conference, Danvers, Mass., Aug. 11-13, 1980; submitted Sept. 16, 1980; revision received May 18, 1981.

*Research Assistant, Department of Aeronautics/Astronautics, now MTS at TRW Redondo Beach, Calif. Member AIAA.

†Professor, Department of Aeronautics/Astronautics. Fellow AIAA.

‡Adjunct Professor, Department of Physics.

§Senior Research Engineer, Department of Aeronautics/Astronautics. Member AIAA.

Measurement Model

The measurement model shown below was used in our analysis:

$$\begin{bmatrix} y_1 \\ y_2 \end{bmatrix} = \begin{matrix} C_1 \\ C_2 \end{matrix} \begin{bmatrix} \cos\varphi & \sin\varphi \\ -\sin\varphi & \cos\varphi \end{bmatrix} \begin{bmatrix} \text{EW} \\ \text{NS} \end{bmatrix} + \begin{bmatrix} v_1 \\ v_2 \end{bmatrix} \tag{1}$$

where y_1 and y_2 are the measurements of spin-axis orientations given by two orthogonal SQUID magnetometers; C_1 and C_2 are the scale factors associated with the two magnetometers; φ is the roll angle of the satellite; v_1 and v_2 are the noise in each of the magnetometer measurements; and EW and NS are the angular differences between the guide star and the gyro spin axis in inertial axes.

The states are C_1, C_2, φ, EW, and NS. After linearizing around the nominal values (indicated by the subscript N)

$$\begin{bmatrix} \delta y_1 \\ \delta y_2 \end{bmatrix} = [H] \begin{bmatrix} \delta\text{EW} \\ \delta\text{NS} \\ \delta\varphi \\ \dfrac{\delta C_1 + \delta C_2}{2} \\ \dfrac{\delta C_1 - \delta C_2}{2} \end{bmatrix} + \begin{bmatrix} v_1 \\ v_2 \end{bmatrix} \tag{2}$$

where

$$H^T = \begin{bmatrix} \cos\varphi & -\sin\varphi \\ \sin\varphi & \cos\varphi \\ -\sin\varphi\text{EW}_N + \cos\varphi\text{NS}_N & -\cos\varphi\text{EW}_N - \sin\varphi\text{NS}_N \\ \cos\varphi\text{EW}_N + \sin\varphi\text{NS}_N & -\sin\varphi\text{EW}_N + \cos\varphi\text{NS}_N \\ \cos\varphi\text{EW}_N + \sin\varphi\text{NS}_N & \sin\varphi\text{EW}_N - \cos\varphi\text{NS}_N \end{bmatrix}$$

The reason for using $(\delta C_1 + \delta C_2)/2$ and $(\delta C_1 - \delta C_2)/2$ will be apparent shortly. Assuming, $E(v_1^2) = E(v_2^2) = \sigma^2$ and $E(v_1 v_2) = 0$. The information form of the standard Kalman measurement update equation gives

$$I_{M+1} = I_M + H_M^T R_M^{-1} H_M$$

where

$$H_M^T R_M^{-1} H_M = \frac{1}{\sigma^2}$$

$$\times \begin{bmatrix} 1 & 0 & \text{NS}_N & \text{EW}_N & (\cos^2\varphi - \sin^2\varphi)\text{EW}_N + \sin\varphi\cos\varphi \text{ terms} \\ & 1 & -\text{EW}_N & \text{NS}_N & (\sin^2\varphi - \cos^2\varphi)\text{NS}_N + \sin\varphi\cos\varphi \text{ terms} \\ & & \text{EW}_N^2 + \text{NS}_N^2 & \sin\varphi\cos\varphi \text{ terms} & 2(\cos^2\varphi - \sin^2\varphi)\text{EW}_N\text{NS}_N \\ & & & \text{EW}_N^2 + \text{NS}_N^2 & 0 \\ & & & & \text{EW}_N^2 + \text{NS}_N^2 \end{bmatrix} \tag{3}$$

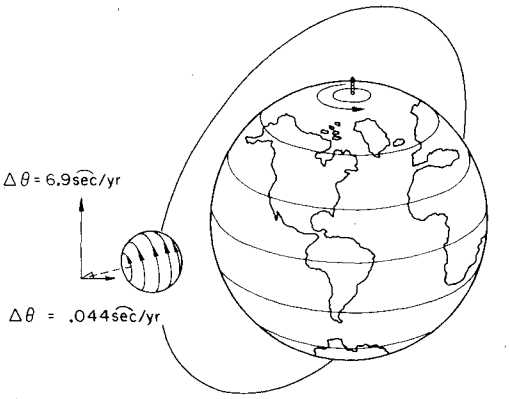

Fig. 1 Relativistic precessions: geodetic and motional.

Table 1 Relativistic precessions

	Angular Drift East
Geodetic:	$A_G\left[t\cos\delta\cos i - \frac{1}{\omega_n}\sin\delta\sin i(\cos\Omega - \cos\Omega_0)\right]$
Motional:	$-\tfrac{1}{2}A_M\left[t\cos\delta(1+3\cos 2i) - \frac{3}{\omega_n}\sin\delta\sin 2i(\cos\Omega - \cos\Omega_0)\right]$
	Angular Drift North
Geodetic:	$-A_G\frac{1}{\omega_n}\sin i(\sin\Omega - \sin\Omega_0)$
Motional:	$\frac{3}{2\omega_n}A_M\sin 2i(\sin\Omega - \sin\Omega_0)$

Table 2 Relativistic precessions in a polar orbit

	Angular Drift East
Geodetic:	0
Motional:	$(A_M\cos\delta)t$
	Angular Drift North
Geodetic:	$A_G t$
Motional:	0

(all information matrices are symmetric, so entries below the diagonal are omitted). Averaging over roll gives

$$(H^T R^{-1} H)_{\text{av}} = \frac{1}{\sigma^2}\begin{bmatrix} 1 & 0 & \text{NS}_N & \text{EW}_N & 0 \\ & 1 & -\text{EW}_N & \text{NS}_N & 0 \\ & & \text{EW}_N^2+\text{NS}_N^2 & 0 & 0 \\ & & & \text{EW}_N^2+\text{NS}_N^2 & 0 \\ & & & & \text{EW}_N^2+\text{NS}_N^2 \end{bmatrix} \tag{4}$$

Thus, $(\delta C_1 - \delta C_2)/2$ is uncoupled from the other states and need not be considered further in the analysis. Denoting $(\delta C_1 + \delta C_2)/2$ by $\delta\overline{C}$, Eq. (4) becomes

$$(H^T R^{-1} H)_{\text{av}} = \frac{1}{\sigma^2}\begin{bmatrix} 1 & 0 & \text{NS}_N & \text{EW}_N \\ & 1 & -\text{EW}_N & \text{NS}_N \\ & & \text{EW}_N^2+\text{NS}_N^2 & 0 \\ & & & \text{EW}_N^2+\text{NS}_N^2 \end{bmatrix}$$

associated with

$$\begin{bmatrix} \delta\text{EW} \\ \delta\text{NS} \\ \delta\varphi \\ \delta\overline{C} \end{bmatrix} \tag{5}$$

The nominal quantities NS_N and EW_N contain, in addition to the slow relativistic drifts and other slow effects to be described below, aberration in the apparent star direction due to 1) the velocity of motion around the sun (annual aberration) and 2) the velocity of orbital motion around the Earth (orbital aberration). These aberrations are sufficiently accurately known to aid substantially in determining scale factor and roll phase errors.

Next the average per orbit of the roll-averaged information matrix, $(H^T R^{-1} H)_{\text{av}}$, is considered.

Before obtaining this, write

$$\text{NS} = \text{NS}' + \Delta(\text{NS})_{\text{orb}} \qquad \text{EW} = \text{EW}' + \Delta(\text{EW})_{\text{orb}} \tag{6}$$

where the orbital aberration components are

$$\Delta(\text{NS})_{\text{orb}} = b\left[\cos nt\frac{\sin i\cos\Omega}{\cos\alpha} + \sin nt(\cos i\cos\delta - \sin\delta\sin i\sin\Omega)\tan\alpha\right]$$

$$\Delta(\text{EW})_{\text{orb}} = b\left[\cos nt\frac{\cos i\cos\delta - \sin\delta\sin i\sin\Omega}{\cos\alpha} - \sin nt\sin i\cos\Omega\tan\alpha\right] \tag{7}$$

where α is the angle between the line of sight to the star and the orbital plane; i is orbit inclination; δ is the star's declination; Ω is the right ascension of the orbit's ascending node relative to that of the star; and t is the time measured from the point on the orbit closest to the star. For orbital altitude 520 km, $b \cong 5$ arcsecond. Note that, if $\cos\alpha > [1-(R_\oplus/a)^2]^{1/2}$, there is occultation of the star by the Earth for part of the orbit, the half occultation angle being in general

$$\theta = \begin{cases} \cos^{-1}\sqrt{1-\left(\frac{R_\oplus}{a}\right)^2}\Big/\cos\alpha & \text{if } \cos\alpha > \sqrt{1-\left(\frac{R_\oplus}{a}\right)^2} \\ 0 & \text{otherwise} \end{cases} \tag{8}$$

α is related to i,δ,Ω by

$$\alpha = \sin^{-1}(\cos i\sin\delta + \cos\delta\sin i\sin\Omega) \tag{9}$$

The doubly-averaged information matrix is

$$(H^T R^{-1} H)_{\text{av av}} = \frac{1}{\sigma^2}\begin{bmatrix} f & 0 & \text{NS}_{\text{av}} & \text{EW}_{\text{av}} \\ & f & -\text{EW}_{\text{av}} & \text{NS}_{\text{av}} \\ & & (\text{EW}^2+\text{NS}^2)_{\text{av}} & 0 \\ & & & (\text{EW}^2+\text{NS}^2)_{\text{av}} \end{bmatrix} \tag{10}$$

where

$$f = 1 - \frac{\theta}{\pi}$$

$$\text{NS}_{\text{av}} = f\,\text{NS}'_N + \frac{b}{\pi}\left(\frac{\sin i\cos\Omega}{\cos\alpha}\right)\sin\theta$$

$$\text{EW}_{\text{av}} = f\,\text{EW}'_N + \frac{b}{\pi}\left(\frac{\cos i\cos\delta - \sin\delta\sin i\sin\Omega}{\cos\alpha}\right)\sin\theta$$

$$(\text{EW}^2+\text{NS}^2)_{\text{av}} = f[\text{EW}'^2_N + \text{NS}'^2_N] + \frac{2b}{\pi}\text{EW}'_N\left(\frac{\cos i\cos\delta - \sin\delta\sin i\sin\Omega}{\cos\alpha}\right)\sin\theta + \frac{2b}{\pi}\text{NS}'_N\left(\frac{\sin i\cos\Omega}{\cos\alpha}\right)\sin\theta + b^2(1+\sin^2\alpha)\frac{f}{2} + \frac{b^2}{4\pi}(\sin^2\alpha - 1)\sin 2\theta$$

Next, consider the dependence of the "slow" variables EW′ and NS′ on relativistic and other slow effects.

$$EW' = EW_0 + (A\cos\delta)t - \frac{B}{\omega_n}\sin i\sin\delta(\cos\Omega - \cos\Omega_0)$$
$$+\Delta(EW)_{ann} + A_g\left[\frac{3t}{8}\sin 2\delta(1+3\cos 2i) + \frac{3}{2\omega_n}\right.$$
$$\cos 2\delta\sin 2i\times(\cos\Omega - \cos\Omega_0)$$
$$\left. - \frac{3}{8\omega_n}\sin 2\delta\sin^2 i(\sin 2\Omega - \sin 2\Omega_0)\right] \quad (11)$$
$$NS' = NS_0 + (PM)_{NS}t - \frac{B}{\omega_n}\sin i(\sin\Omega - \sin\Omega_0) + \Delta(NS)_{ann}$$
$$+A_g\left[-\frac{3}{2\omega_n}\sin\delta\sin 2i(\sin\Omega - \sin\Omega_0)\right.$$
$$\left. + \frac{3}{4\omega_n}\cos\delta\sin^2 i(\cos 2\Omega - \cos 2\Omega_0)\right]$$

where

$$A = A_G\cos i - \tfrac{1}{2}A_M(1+3\cos 2i) + (PM)_{EW}/\cos\delta$$
$$B = A_G - 3A_M\cos i$$

Here the A_g term is due to the Earth's gravity gradient torque on the unavoidably slightly oblate spinning spherical gyro. A_g also includes the precession due to a small suspension torque if the gyro is displaced from the satellite's mass center along the roll axis (displacements perpendicular to the roll axis produce torques which average out during a roll period). The coefficient A_g is not accurately known a priori, but is distinguishable from the other effects in EW′ and NS′ because of the second harmonic in Ω (assuming that the inclination i is sufficiently different from 90 deg so that Ω varies appreciably during the mission).

$(PM)_{NS}$ and $(PM)_{EW}$ are the constant proper motion of the guide star, not very accurately known. Note that $(PM)_{NS}$ is distinguishable from B in its effect on NS′ (again assuming that Ω varies appreciably), whereas $(PM)_{EW}$ is an inseparable part of A. $\Delta(EW)_{ann}$ and $\Delta(NS)_{ann}$ are the annual aberration of Rigel

$$\Delta(EW)_{ann} = -20.426 \text{ arcsecond } \cos(\theta_\odot + \epsilon)$$
$$\Delta(NS)_{ann} = 10.426 \text{ arcsecond } \sin(\theta_\odot + \epsilon)$$
$$- 1.404 \text{ arcsecond } \cos(\theta_\odot + \epsilon) \quad (12)$$

where $\theta_\odot$ is the celestial longitude of the sun relative to Rigel and ϵ is a small phase shift due to the parallax of Rigel, assumed to be 2×10^{-4} rad with some a priori uncertainty. The unknown parameters affecting our averaged measurements are thus $\delta\varphi$, $\delta\overline{C}$, $\delta(EW)_0$, $\delta(NS)_0$, δA, δB, δA_g, $\delta(PM)_{NS}$ and $\delta\epsilon$.

If all nine parameters could be regarded as constant during the mission, it would be a simple matter to sum the averaged information (10), now interpreted relative to the nine parameters, together with any desired a priori information (the inverse of an a priori covariance matrix) to determine the a posteriori covariance, for example, of the quantities δA and δB. In summing the information (10), the time step may be taken to be several orbital periods rather than a small fraction of a roll period, provided of course that the measurement variance σ^2 is reduced in inverse proportion to the time step. Since

$$A_M = A - B\cos i - (PM)_{EW}/\cos\delta$$
$$A_G = 3A\cos i - \frac{B}{2}(1+3\cos 2i) - 3(PM)_{EW}\cos i/\cos\delta \quad (13)$$

the uncertainties in the determination of the quantities A_M and A_G can be obtained, provided a suitable a priori uncertainty is associated with the current astronometric value for $(PM)_{EW}$. In this paper the measurement "biases" $\delta\varphi$, $\delta\overline{C}$ are not assumed strictly constant but are allowed to vary slowly in a random manner:

$$(\delta\varphi)_{M+1} = (\delta\varphi)_M + (w_1)_M$$
$$(\delta\overline{C})_{M+1} = (\delta\overline{C})_M + (w_2)_M \quad (14)$$

where the $(w_i)_M$'s are independent random increments. These "dynamic" evolutions are incorporated into a standard Kalman covariance evolution:

Measurement update:

$$P_M^+ = P_M^- - P_M^- H_M^T(H_M P_M^- H_M^T + R_M)^{-1} H_M P_M^-$$

Time update:

$$P_{M+1}^- = P_M^+ + \begin{bmatrix} 0 & & & & \\ & 0 & & & \\ & & \ddots & & \\ & & & q_1 & \\ & & & & q_2 \end{bmatrix} \quad (15)$$

where q_i is the variance of $(w_i)_M$.

Results

The purpose of the error analysis is to compute the expected error in measuring the relativistic precessions (i.e., A_G and A_M). This was accomplished by implementing a Kalman filter covariance analysis on the computer using the model previously discussed. The averaging technique reduced the amount of computer time needed by a factor of ~1000 compared to the time required without averaging.

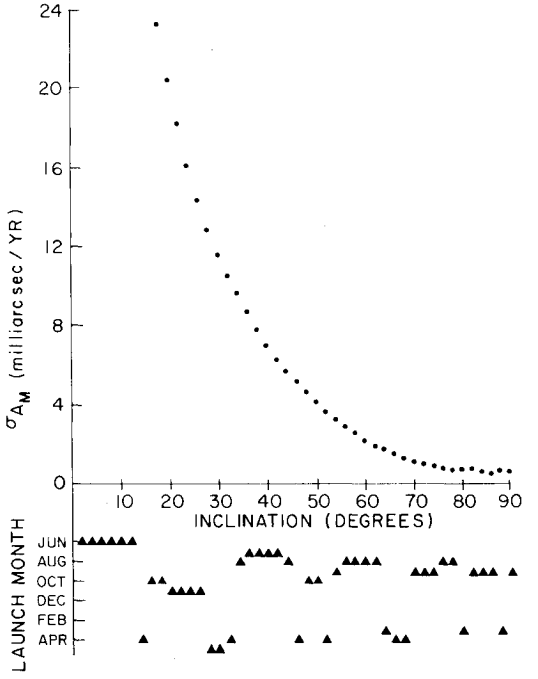

Fig. 2 Expected error in the motional precession with proper motion assumed known, inclinations from 0 deg to 90 deg.

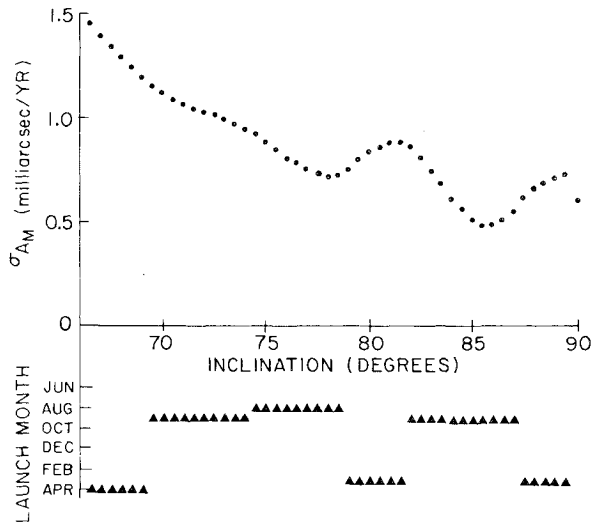

Fig. 3 Expected error in the motional precession with proper motion assumed known, inclinations from 66 deg to 90 deg.

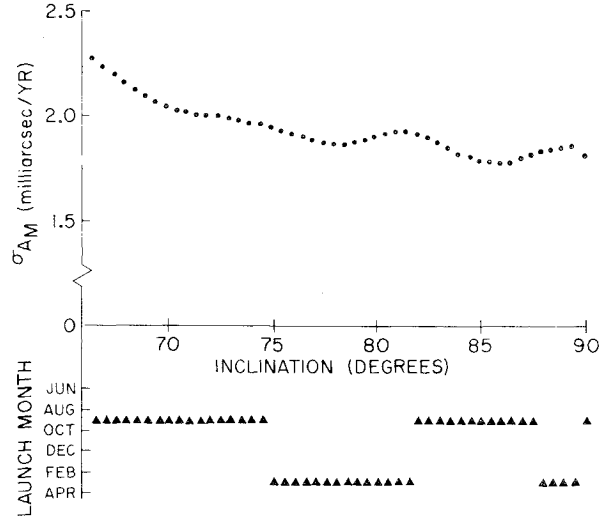

Fig. 4 Expected error in the motional precession with typical proper motion uncertainties.

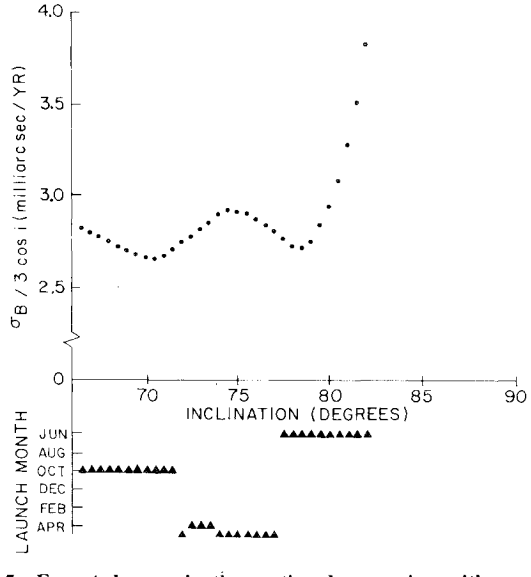

Fig. 5 Expected error in the motional precession with pessimistic proper motion uncertainties.

Table 3 Results of investigation

Proper motion uncertainty, milliarcsecond/year	i, deg	Month of launch	Expected error in A_M, milliarcsecond/year
No uncertainty	85.5	Sept.	0.49
NS = 0.9, EW = 1.7	85.5	Sept.	1.79
NS = 9.0[a]	70.5	Oct.	2.67

[a] A_G is assumed equal to theoretical value.

All studies assumed the following: a 1-year mission; time step $\Delta t = 0.01$ year; measurement noise $\sigma = 0.8936$ milliarcsecond; a random drift in $\bar{C}$ of 0.01% during the year $\Rightarrow q_1 = 10^{-10}$; and a random drift in φ of 2 arsecond during the year $\Rightarrow q_2 = 0.04$ arcsecond^2.

The a priori uncertainties in the states other than the proper motions were conservatively large: $\sigma_A = \sigma_B = 30$ arcsecond/year; $\sigma_{A_g} = 30$ milliarcsecond/year; $\sigma_{(\mathrm{NS})_0} = \sigma_{(\mathrm{EW})_0} = 30$ arcsecond; $\sigma_{\bar{C}} = 10^{-3}$(nominal $\bar{C}$ being 1); $\sigma_\epsilon = 0.001$ rad; $\sigma_\varphi = 20$ arcsecond; the initial node relative to Rigel is chosen so that Rigel is in the orbit plane halfway through the mission; and different a priori uncertainties in the proper motion of Rigel were assumed in the following studies.

Three studies were carried out with different assumptions on proper motion:

1) The first study was made assuming the proper motion of Rigel was known exactly (i.e., $\sigma_{(\mathrm{PM})_{\mathrm{NS}}} = 0$, $\sigma_{(\mathrm{PM})_{\mathrm{EW}}} = 0$). Inclinations every 2 deg between 0 and 90 deg were studied with 12 launch dates considered for each inclination. The expected error in measuring the relativistic precessions depends on the launch date because the phase of the annual aberration varies with the time of year of launch. For each inclination the launch date was chosen to minimize the expected error, σ_{A_M}, in measuring the motional precession since the predicted motional precession is much smaller than the predicted geodetic precession. Figure 2 shows the results under the assumption that the proper motion of Rigel is known exactly. It shows that the expected error is smallest for inclinations between 70 and 90 deg. A more detailed view of this region is shown in Fig. 3. This shows two local minima at approximately 78 and 85.5 deg. For these inclinations the node regresses a little more than 540 deg (3π) and 180 deg (π), respectively, in 1 year. Thus, at the beginning and end of the year, the orbit plane is nearly perpendicular to the line of sight to Rigel. So the star is not occulted by the Earth at those times, which are the most important for determining the slope of a straight line (i.e., a linear drift). Hence, the advantage to be gained in going to a slightly off-polar orbit.

2) Using the latest astronometric data, the present uncertainty in NS proper motion and EW proper motion are 0.9 and 1.7 milliarcsecond/year, respectively.[9] Inputting these values as the a priori uncertainties in proper motion to the computer program gave the results shown in Fig. 4. Inclinations of 78.5 and 85.5 deg are local minima, but σ_{A_M} is 1.88 and 1.79 milliarcsecond/year, respectively compared to 0.728 and 0.485 milliarcsecond/year obtained assuming proper motion was known exactly.

3) What if the error in Rigel's proper motion is a factor of 10 larger than the uncertainty computed from the accepted astronometric data? Then, the uncertainty in any linear term would be much larger than the milliarcsecond/year level, due to the proper motion errors alone. But, there is one combination of relativistic terms in an inclined off-polar orbit, that is sinusoidal in the longitude of the node, and could theoretically be separated from the proper motion error. This combination is $B \triangleq A_G - 3A_M \cos i$ (see Table 1). Furthermore, if the measurements show the geodetic term to be very nearly correct, then the true value of A_G might be assumed equal to its Einstein value and the measured value of B could be used

to compute A_M:

$$(A_M)_{\text{meas}} = \frac{(A_G)_{\text{Einstein}} - (B)_{\text{meas}}}{3\cos i}$$

Pursuing this idea further gives

$$\sigma_{A_M} = \sigma_B / 3\cos i$$

σ_B is obtained with a pessimistic assumption on uncertainty in NS proper motion (10 times the present value) in the computer program, producing the results shown in Fig. 5. A polar orbit is obviously no good for this case. Local minima occur at inclinations of 70.5 and 78.5 deg. These inclinations result in orbit plane regressions of approximately 900 deg (5π) and 540 deg (3π), respectively.

Conclusions

Table 3 summarizes the results for this investigation, by choosing the best orbit (i.e., minimum σ_{A_M}) under each assumption about proper motion.

The final decision on which orbit to use will depend on which assumption seems to be the wisest as launch time approaches:

1) new measurements have reduced the proper motion uncertainty to near zero;

2) proper motion uncertainties derived from the current astronometric data are the most realistic;

3) take the conservative viewpoint that proper motion may not be as accurately known as presently believed.

It should be pointed out that the results presented in this paper are somewhat optimistic because changes in the scale factor due to temperature fluctuations in the electronics and some torques produced by the suspension system have not been included in the model.

Acknowledgment

The support of NASA Contract NAS8-32605 is acknowledged.

References

[1] Schiff, L.I., "Possible New Experimental Test of General Relativity Theory," *Physics Review Letters,* Vol. 4, March 1, 1960, pp. 215-217.

[2] Schiff, L.I., "Motion of a Gyroscope According to Einstein's Theory of Gravitation," *Proceedings National Academy of Sciences,* Vol. 46, April 19, 1960, pp. 871-882.

[3] Everitt, C.W.F., "The Gyroscope Experiment I: General Description and Analysis of Gyroscope Performance," *Experimental Gravitation,* edited by B. Bertotti, Academic Press, New York, 1973, pp. 331-360.

[4] Lipa, J.A., Fairbank, W.M., and Everitt, C.W.F., "The Gyroscope Experiment II: Development of the London-Movement Gyroscope and of Cryogenic Technology for Space," *Experimental Gravitation,* edited by B. Bertotti, Academic Press, New York, 1973, pp. 361-380.

[5] Lipa, J.A. Nikirk, J.R., Anderson, J.T., and Clappier, R.R., "A Superconducting Gyroscope for Testing General Relativity," *Low Temperature Physics LT-14,* edited by Matti Krusius and Matti Vuorio, Vol. 4, North Holland/American Elsevier, New York, 1975, pp. 250-258.

[6] Anderson, J.T. and Cabrera, B., "Integration of SQUID $1/f$ Noise and Its Application to a Superconducting Gyroscope," *Journal de Physique,* Vol. 39, 1978, pp. C6-1210-C6-1212.

[7] Everitt, C.W.F., "A Superconducting Gyroscope to Test Einstein's General Theory of Relativity," *Society of Photo-Optical Instrumentation Engineers Proceedings,* Bellingham, Washington, 1979, pp. 175-188.

[8] "Report on a Program to Develop a Gyro Test of General Relativity in a Satellite and Associated Control Technology," Stanford University, June 1980.

[9] Anderson, J.T. and Everitt, C.W.F., "Limits on the Measurement of Proper Motion and the Implications for the Relativity Gyroscope Experiment," Physics Department, Stanford University, 1979, unpublished report.